HiSST: International Conference on
High-Speed Vehicle Science Technology
26–29 November 2018, Moscow, Russia

Aerodynamic characteristics of generic test models under high-temperature real-gas condition in free-piston shock tunnel HIEST

TANNO Hideyuki, KOMURO Tomoyuki, SATO Kazuo and ITOH Katsuhiro Author[1]

Abstract

A series of wind tunnel test campaigns conducted in the HIEST free-piston high-enthalpy shock tunnel were reported. Three-component aerodynamic characteristics (drag, lift and pitching moment) with generic test models; blunted cone, capsule and lifting body, were measured under high-temperature real-gas condition. A free-flight multi-component force-measurement technique was implemented, which involved the test model being completely non-restrained for the duration of the test and thus experiencing free-flight conditions for a period in the order of milliseconds. Compared with conventional force measurement techniques, the present one has the advantage of no aerodynamic and mechanical interference with the model support system and less variation in the model position and attitude during the test resulting high-precision measurement. Through the comparison between under perfect gas and high-temperature real-gas condition, it was found that drag and lift coefficients agreed well with all the test models. On the contrary, pitching moment coefficient differed significantly, in particular with the lifting body.

Keywords : *High-temperature real-gas, aerodynamics, shock tunnel*

Nomenclature

AOA	=	Angle of attack	PI	=	Prediction interval
C_A	=	Axial force coefficient	X	=	Model displacement (x-direction)
C_N	=	Normal force coefficient	Y	=	Model displacement (y-direction)
C_D	=	Drag force coefficient	σ	=	Standard deviation
C_L	=	Lift force coefficient			
C_{My}	=	Pitching moment coefficient			
P_0	=	Stagnation pressure			
P_{Pitot}	=	Free-stream Pitot pressure			

1. Introduction

Aerodynamic characteristic particularly pitching stability during hypersonic gliding phase is still one of the crucial matters for the design of re-entry vehicles. In the first flight of the Space Shuttle, unexpected pitch-up was found during the Hypersonic gliding phase. The body-flap deflection angle for pitch trim had to be almost twice that predicted in the prefight wind-tunnel tests. Post-flight analysis implied that high-temperature real-gas effects[1-3] were one of the major causes of this deflection-angle discrepancy. The high-temperature real-gas effect, which produces pressure distribution around the vehicles differs from those of perfect-gas flow. It introduces a significant forward-shift of the pressure center of the vehicles and consequently leads pitching moment remarkably higher than that of predicted in the conventional wind tunnels. In order to duplicate this high-temperature real-gas effect in the ground test facilities, both high stagnation temperature and high stagnation pressure (namely density) are required because the effect strongly depends on the dissociation of molecules in the test free-stream (Binary scaling). However, only available Hypersonic facilities which can produce the high temperature and high-pressure condition above are impulse facilities, which test duration is extremely short as an order of the millisecond. Due to its short test duration, the measurement of aerodynamic

[1] *Japan Aerospace Exploration Agency, Kakuda Space Center,Kakuda Miyagi 981-1525 JAPAN, tanno.hideyuki@jaxa.jp*

forces present significant technical difficulties compared with conventional wind tunnels. One of the major technical issues encountered was mechanical vibration principally from the model supporting system such as sting or stand, which mechanical vibrations were not damped out within the milliseconds of the test duration, resulting in large-scale oscillations in the measured signals. This problem degrades the time response that the measurement precision in particular pitching moment is insufficient to detect the high-temperature real gas effect.

Fig 1. Free-piston shock tunnel HIEST.

In JAXA Kakuda Space Centre, we have been studying Hypersonic aerodynamics includes force measurement technique in our free-piston shock tunnel HIEST[4](Fig.1). This tunnel can be operated at stagnation pressures up to 150 MPa and stagnation enthalpies up to 25 MJ/kg, under which conditions test time of 2 milliseconds or longer is attainable. In 2010, the novel force measurement technique based on free-flight test method was developed for the facility [5]. In the technique, the model is released down from a magnetic holder installed on the wind-tunnel ceiling so that it lies in the nozzle core flow synchronized with the arrival of the test flow. During the entire test duration, the model is thus completely unrestrained by any support system and therefore free both aerodynamically and mechanically. Since the test model is free from aerodynamic interference and from vibration issues, remarkable improvement of the measurement accuracy and precision can be hence expected with the technique.

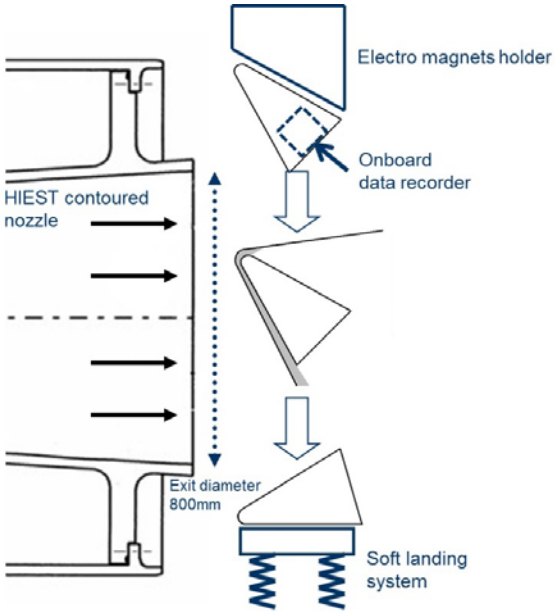

Fig 2. The 'Free-flight force measurement technique'

The present article described the aerodynamic characteristics of the three typical re-entry configurations measured with the free-flight technique under the high-temperature real-gas condition in HIEST. First, we provide details of the technique: a miniature onboard data-recorder, the test model and the model releaser-catcher. Following the discussion on the accuracy and precision of the measurements of the three-component aerodynamic characteristics with reference to experiments on a blunted cone, the previously documented real-gas effect on aerodynamics, namely an increased trim angle tendency in the pitch, can be experimentally verified by comparing low- and high-enthalpy test conditions (i.e. perfect- and real-gas conditions). To determine the trim angle of the HTV-R re-entry capsule and HYFLEX lifting body on re-entry, series of HIEST test campaigns under high-temperature real-gas conditions were also conducted.

2. Free-flight force measurement technique in shock tunnels

Free-flight force-measurement techniques have been implemented by previous researchers; a good summary can be found in Bernstein[6]. Most previous work was based on optical measurements using a high-speed camera system. Displacements are obtained directly from test-model images, whereupon accelerations are derived through double-differentiation of the displacement curves. Moreover, this differentiation significantly amplifies the measurement noise and since measurement accuracy of

depends on the model displacement, lightweight models are generally favored. This, however, can lead to variations in the model position and angle of attack during the test. To improve measurement accuracy, Naumann et al.[7] used direct acceleration measurements with miniature accelerometers mounted inside the model in experiments carried out in a shock tunnel. Through a cleverly designed model injection and catching system, the test model could experience free-flight conditions over 10 milliseconds. Nevertheless, the model injection system and umbilical to the rear of the model may have generated aerodynamic interference with the model wake flow; such interference would become particularly undesirable if pitching-moment measurements were required at high angles of attack.

In the present free-flight technique, the model is released from a magnetic releaser installed on the wind-tunnel ceiling so that it lies in the nozzle core synchronized with the arrival of the test flow. Throughout the entire test, the model is thus completely unrestrained by any support system and both aerodynamically and mechanically unhindered. Since a comparatively heavy model can be applied using this technique, variation in model position and attitude can be virtually eliminated during the test period of high dynamic pressure in HIEST. Moreover, acceleration measurement accuracy can be ensured with on-board accelerometers, the outputs of which were stored on an on-board miniature data recorder. Upon conclusion of the test flow, the model falls into a soft-landing system placed on the floor, enabling the model and instruments to be reused. This sequence of events is shown in Fig. 2.

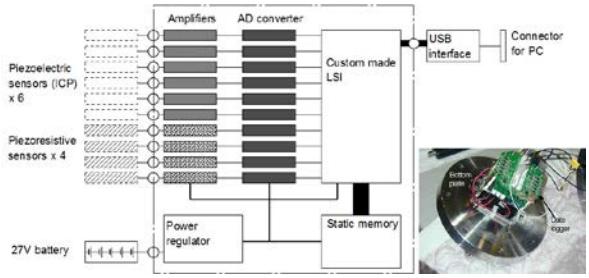

Fig 3. Block diagram of the onboard data-recorder

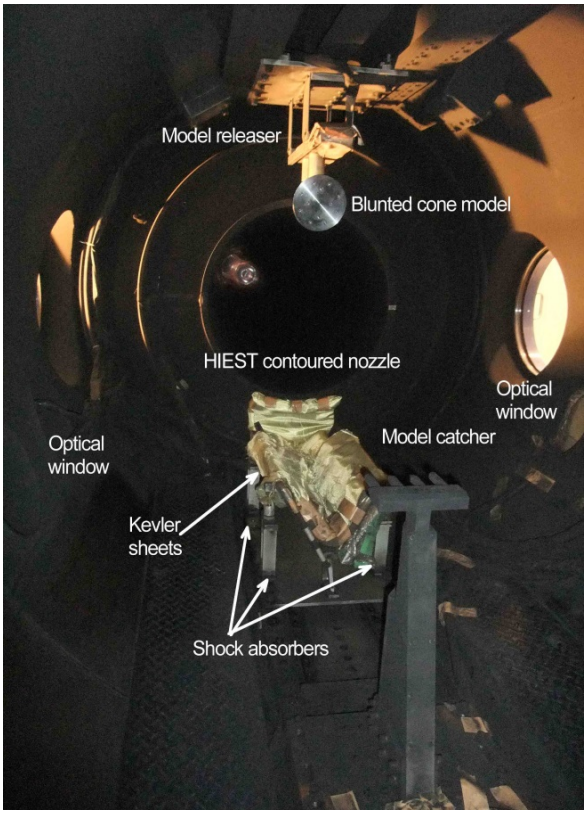

Fig 4. The Model releaser and catcher in the HIEST test section.

3. Wind tunnel test set-up

3.1. Miniature data recorder

An on-board miniature data-recorder is the key technology for the present ‘free-flight’ aerodynamic measurements. In determining aerodynamic forces and moments with acceleration measurements, since two accelerometers are required for the force and moment on each axis, at least six accelerometers are necessary for six-component measurements. Moreover, recording the free-stream Pitot pressure is also crucial, to be able to normalize forces and obtain aerodynamic coefficients. The recorder should thus be designed to accommodate six channels of piezoelectric sensors (PCB Piezotronics Inc. ICP-type sensors) for accelerometers and a few channels of piezoresistive sensors (Kulite Semiconductor Products, Inc.) to measure pressure. Since the test time in HIEST is in the order of milliseconds, a high sampling rate of 500 kHz is crucial and measurement accuracy of 16 bits is also required to guarantee sufficient accuracy. In addition, the recorder includes batteries with sufficient storage to ensure run time of 2 hours, although these must also be sufficiently compact to mount within the limited space inside the model.

Unfortunately, no commercially available data-recorder currently satisfies these requirements. Accordingly, an original data recorder was designed and manufactured at JAXA[5]. As shown in the circuit diagram of the recorder (Fig. 3), a custom-made LSI reads the measured signal from the A/D converter and stores digitized data in static memory. The recorder was designed to maximize operating speed and minimize size: a four-layer circuit board was adopted, which resulted in recorder dimensions of 100 (L) x 100 (W) x 70 mm (H). The total measurement time of the recorder is 800 milliseconds, which is determined by the onboard memory capacity. The recorder also has a pre-trigger system, which can be arbitrarily adjusted with micro-switches, while to arm the trigger, the recorder has an IR photo switch and an LED indicator showing the status of the recorder. After each wind-tunnel test, data stored in the static memory of the recorder were transferred to a host PC through a USB interface.

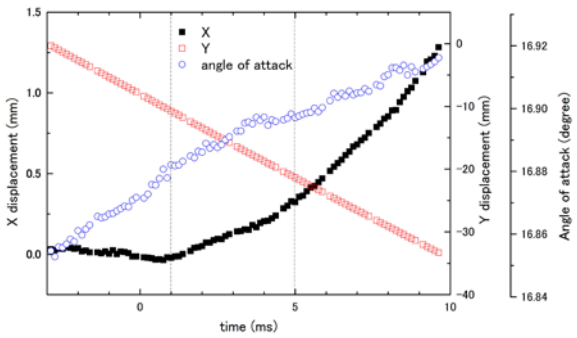

Fig 5. X, Y displacements and angle of attack of the model recorded during a typical experiment The dashed vertical lines indicate the approximate steady test time

3.2. Test models

The three generic test models (blunted cone, capsule and lifting body) were applied in the series of the test campaigns. As will be described shortly in the previous section, high-power electromagnets on the ceiling of the HIEST test section were used to hold and release the model. There were concerns that the intense magnetic field produced by electromagnets might interfere with the electrical components of the data-recorders inside the model. Accordingly, all the test models were manufactured from a ferromagnetic material, namely stainless steel SUS410, which functioned as a shield and prevented the electromagnetic field from penetrating the model. The total mass of the test models were 17kg to 20 kg, including the internal instrumentation, which comprised a data recorder with batteries, sensors (piezoelectric accelerometers and piezoresistive pressure transducers). The specifications of each test models were tabulated in Table.1. Theoretically, this would enable six-component force measurement, although only three components were measured in these test campaigns. Two accelerometers were configured to measure each of these aerodynamic components. The pressure transducers were mounted vicinity of the model nose to obtain free-stream Pitot pressure as the basis for calculating aerodynamic coefficients.

Table 1. Test model specifications

	Blunted cone	**Capsule**	**Lifting body**
Total mass (kg) (including sensors and data recorders)	19.75	20.13	16.78
Moment of inertia Iyy (kgm^2)	0.1515	0.130	0.226
Total length (mm)	316	195.6	0.440
Diameter (mm)	200.0	250.0	N.A
Number of data recorders	1	2	3
Accelerometers (Piezoelectric)	6	12	16
Pressure transducers (Piezoresistive)	2	4	8

Table 2.

Free-stream condition of HIEST low-enthalpy (perfect-gas), high-enthalpy (real-gas) and HWT2

		HIEST Low enthalpy	HIEST High enthalpy	JAXA-HWT2	ONERA-S4MA
Stagnation (nozzle reservoir) condition	Pressure (MPa)	1.3×10^{1}	1.5×10^{1}	6.1	8.5
	Temperature (K)	3.0×10^{3}	7.6×10^{3}	1.1×10^{3}	1.1×10^{3}
	Enthalpy (MJ/kg)	3.8	1.6×10^{1}	N.A.	N.A.
Free-stream condition	Temperature (K)	2.9×10^{2}	1.3×10^{3}	5.5×10^{1}	5.4×10^{1}
	Pressure (kPa)	1.1	2.1	1.7×10^{-1}	1.8×10^{-1}
	Density (kg/m³)	1.4×10^{-2}	4.8×10^{-3}	1.1×10^{-2}	1.2×10^{-2}
	Velocity (km)	2.6×10^{3}	4.9×10^{3}	1.5×10^{3}	1.7
	Mach number	7.6	6.2	9.7	9.9
	Unit Reynolds number (/m)	2.0×10^{6}	4.5×10^{5}	3.7×10^{6}	4×10^{6}
	O mass fraction	3.3×10^{-4}	6.9×10^{-2}	N.A.	N.A.
	O2 mass fraction	2.1×10^{-1}	1.4×10^{-1}	N.A.	N.A.

3.3. Model releaser and catcher

As shown in the photographs of the model set-up in the HIEST test section (Fig. 4), a model (blunted cone) is initially suspended by two electromagnets, which were capable of holding 60 kg. Since the test model must lie in the nozzle core flow synchronized with the test flow arrival, the release system must respond rapidly to the trigger signal from tunnel initiation with millisecond-order accuracy. The release system was able to vary the model angle of attack from 0 to 60°. The prototype of the releaser developed in the study was located 400 mm above the axis of the nozzle centre to avoid damage to the magnets from the high-temperature hypersonic test flow, as well as from the high-speed particles often produced as main-diaphragm debris. To adjust the model-release timing, a digital controller was developed to deactivate the electromagnets at a precise time. The controller included a sequencer, electrical relays, and the digital retarder.

Finally, following the test, test models fall to the catcher located at the bottom of the HIEST test section, having reached a final speed of less than 10 m/s. To avoid damaging the model and allow it to be reused, the strength of this impact should be mitigated. The catcher thus includes thus four hydraulic dampers to absorb impact energy, while shock-absorbing polymer sheets were also placed on the catching surface of the system. Furthermore, a data-recorder is installed in the model with an anti-shock mounting. Taking these steps allowed the acceleration of the model and data-recorder on impact to be minimized, facilitating reuse of the complete system throughout the entire measurement campaign.

3.4. Model displacement during free-flight

One of the critical issues encountered in free-flight measurement techniques is the variation in position and attitude of the model during the test. Here, an optical monitoring technique[8, 9] was adopted to observe the model motion, with sequential Schlieren images recorded by a high-

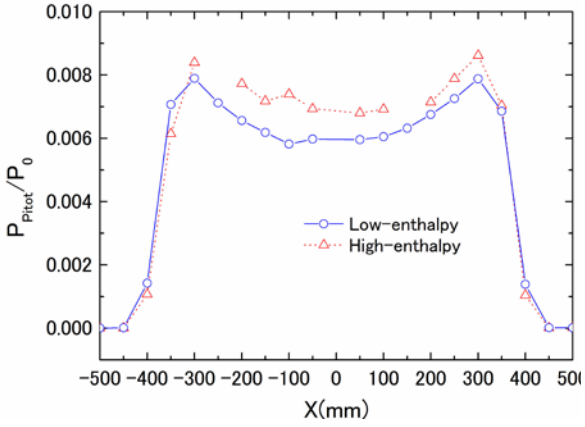

Fig 6. Normalized Pitot pressure profiles obtained in the contoured nozzle calibration shots. The open circles and triangles depict the results obtained under low- and high-enthalpy conditions, respectively

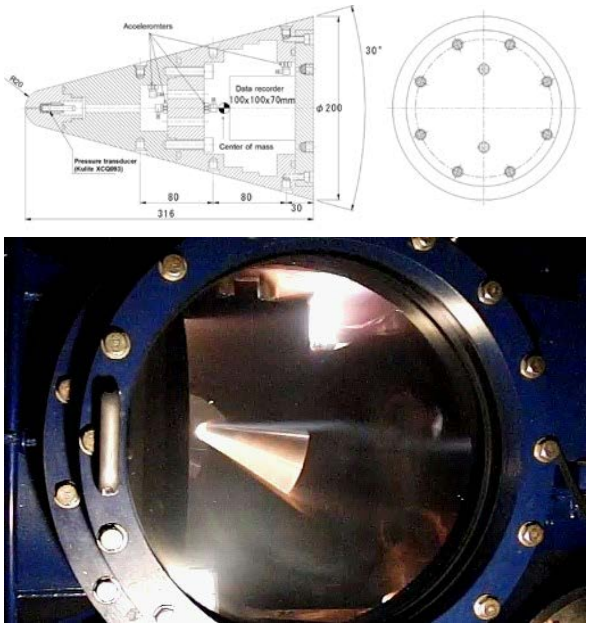

Fig 7. (Top) Schematic of the blunted cone. (Bottom) Sequential images of the model dropping in the HIEST test section coefficients.

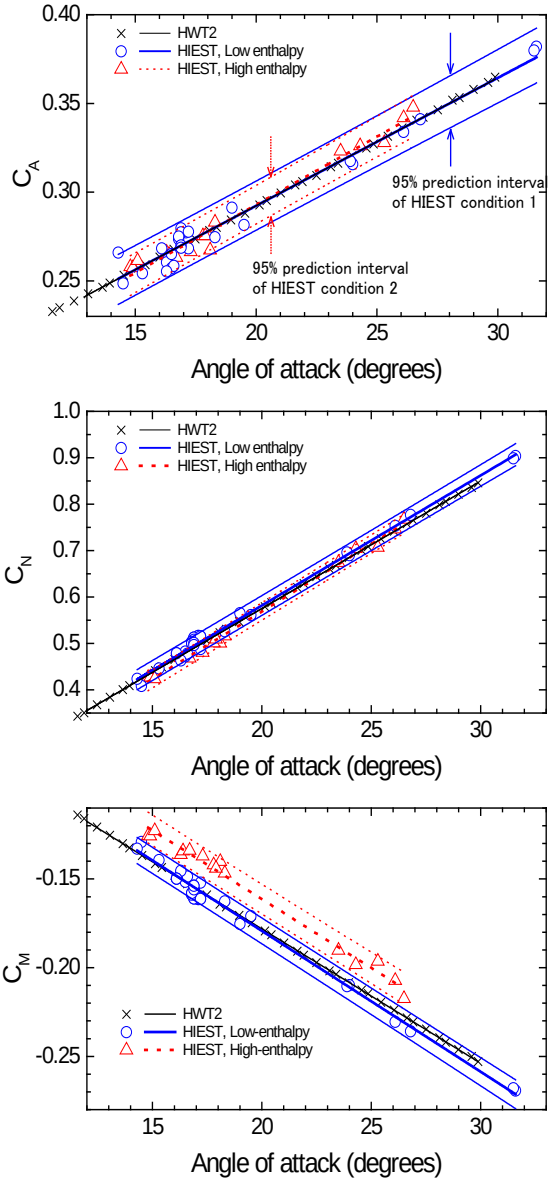

Fig 8. Aerodynamic coefficients C_A(Top), C_N(Middle) and C_M(Bottom) for angles of attack from 14 to 32 degrees. Open circles and triangles (low- and high-enthalpy conditions respectively) show the present measurements with the crosses; providing a comparison with results from the blow-down wind tunnel JAXA-HWT2. 95%-PI (prediction interval) defining the uncertainty limits are also shown in thin lines for HIEST two conditions.

speed video camera (SHIMADZU Corp. Hypervision). An example of typical displacement profiles of a model (blunted cone) in x and y directions, as well as the pitch-angle history, are presented in Fig. 5. Throughout the present test campaign, the standard deviation of the cone location and the angle of attack at the time of the test-flow arrival was maintained at less than ±11 mm from the nozzle centre and less than ±0.4° from the initial angle of attack, respectively.

In previous nozzle-calibration tests, Pitot pressure distributions under both conditions employed were measured as shown in Fig. 6. The calibration test indicated that Pitot pressure deviation from the average value within a 150mm radius of the nozzle centre-line circle under low-enthalpy condition was and for high enthalpy. Based on this free-stream uniformity, the core of the test flow was defined as a 300mm-diameter circle in this test campaign.

4. Test results

4.1. Test flow condition

The HIEST facility has two nozzles, conical and contoured respectively. During this test campaign, we used the contoured nozzle, which has an exit diameter of 800 mm, a nozzle throat of 50 mm, and an area expansion ratio of 256. In all the HIEST test campaigns reported in this article, two tunnel conditions were selected. Table 2 shows the test-flow conditions, which were calculated with an axis-

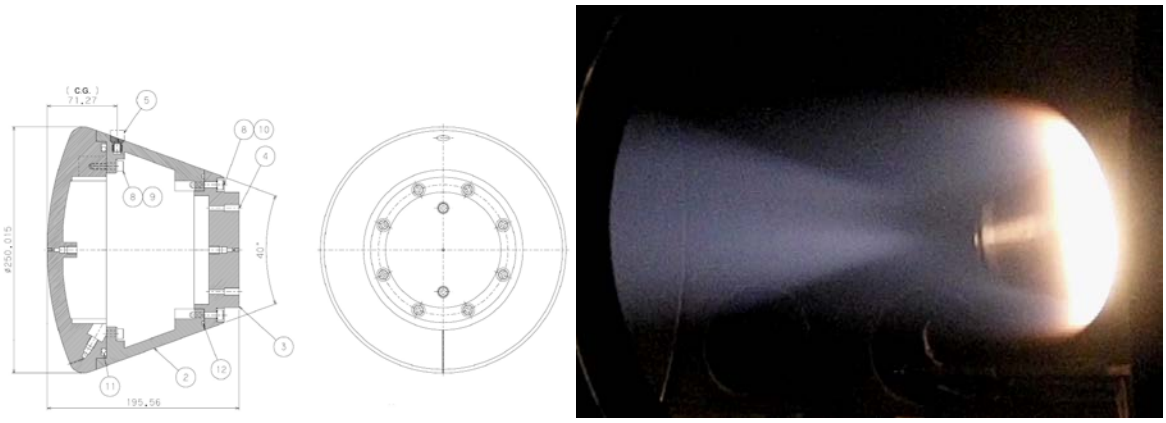

Fig 9. (Left) HTV-R 6% scaled model to measure three-component aerodynamic force. HIEST test section. (Right) HTV-R capsule free-flying in the HIEST test section (under high-enthalpy condition).

symmetrical in-house nozzle flow code[10]. The first condition was low-enthalpy, in which the flow could be approximated as a perfect gas, enabling measurements to be compared directly with results from the conventional blow-down wind tunnel JAXA-HWT2[11] and ONERA-S4MA[12] to evaluate the accuracy of the technique. The second condition was high-enthalpy with 85% dissociation of the oxygen molecule in the reservoir; high-temperature real-gas effects were thus evaluated by comparing with perfect-gas results.

4.2. Blunted cone

At first, to estimate the accuracy and precision of the present free-flight force measurement technique, three-component force measurement with a blunted cone model was conducted. The test model, as shown in Fig. 7, was a 316mm-long blunted cone with a half-angle of 15º, a nose-tip radius of 20 mm and a base diameter of 200 mm. The total mass of the cone was 19.75 kg, including the internal instrumentation.

In Fig. 8, depicted as open symbols show the relationship between aerodynamic coefficients and the angle of attack as the latter is varied from 14 to 32º. Circles and triangles in the figure showed results under low- and high-enthalpy conditions (perfect- and high-temperature real-gas respectively.) Aerodynamic coefficients measured in the blow-down hypersonic wind tunnel HWT2 are also plotted as crosses and used as a baseline under perfect-gas conditions to estimate the accuracy of HIEST measurements. Assuming the variation in each of the aerodynamic coefficients over the angle of attacks from 14 to 32º to be linear, the linear regression method was applied to analyse uncertainty in the present HIEST measurements. In the figures, the thick solid, dotted and thin solid lines depicted the least-square-fitting lines for HIEST low- and high-enthalpy conditions and HWT2. The uncertainty of

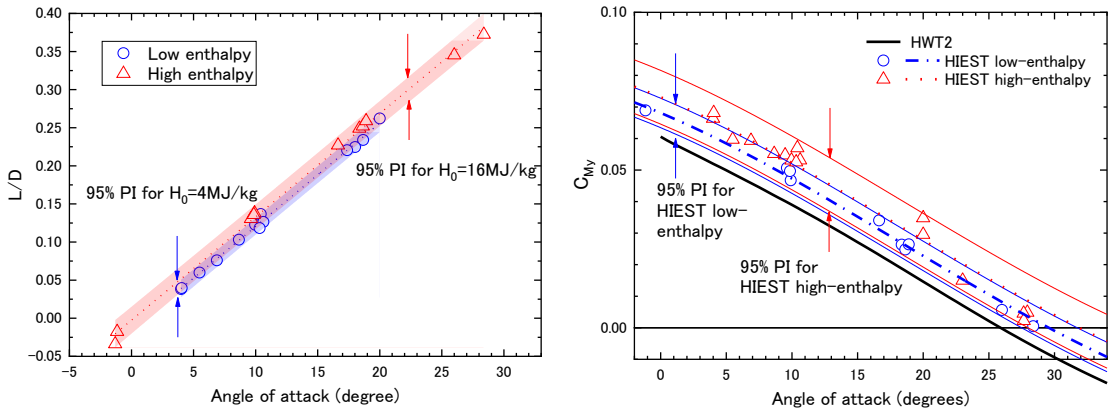

Fig 10. L/D (Left) and C_{My} (Right) profile of the HTV-R capsule at AOA from 0 to 30 degrees.

the measurements is defined as the 95%-PI (prediction interval); plotted as thin lines in the figures as the upper and the lower uncertainty constraints. Since the 95%-PI of the HWT2 results were substantially smaller than those of HIEST, these uncertainty lines are not plotted in the figures.

To estimate the present measurement accuracy, results under HIEST low-enthalpy condition and HWT2 were compared, as both cases could be considered perfect-gas flows. As shown in Fig. 8, the two measurement groups agreed within their constraints, i.e. no significant differences emerged in any of the aerodynamic coefficients (CA, CN and CM). This means we can be confident that the accuracy of the free-flight measurements in HIEST lies within the measurement uncertainties. If we now compare HIEST low- and high-enthalpy conditions, we see that the CA and CN coefficients agree within their respective uncertainties. In contrast, CM for the high-enthalpy condition consistently exceeds that of low enthalpy and since the uncertainties do not overlap, this difference can be considered significant. Since this discrepancy is observed not in CA and CN but only in CM, it is considered attributable to the high-temperature real-gas effect mentioned in the introduction.

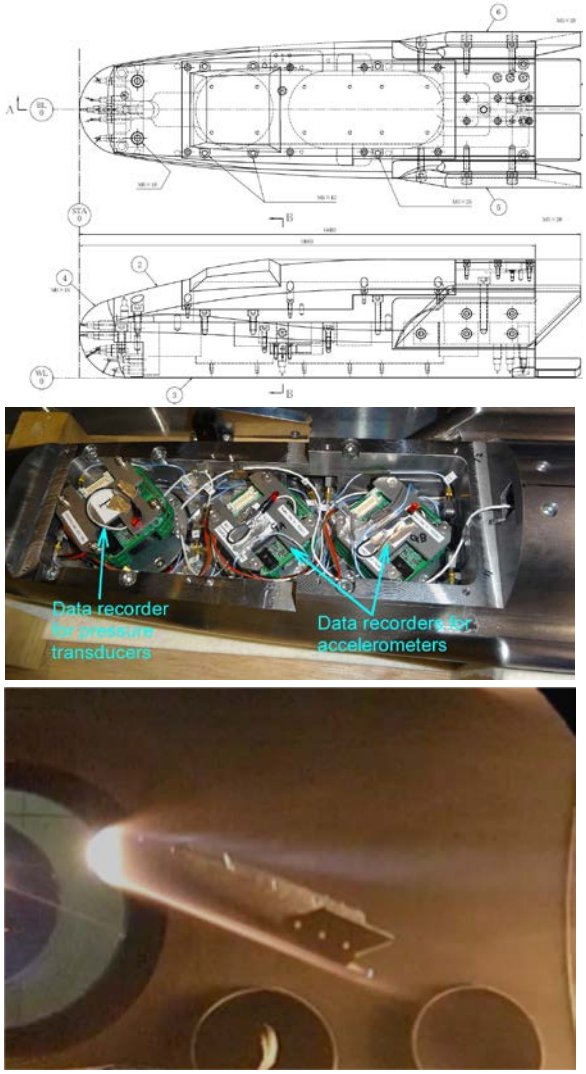

Fig 11. (Top) Schematic of the HYFLEX free-flight test model. (Middle) Three data recorders instrumented in the HYFLEX free-flight model. HYFLEX test model free-flying in a hypersonic free-stream (Low-enthalpy condition).

4.3. Re-entry capsule

JAXA has been researching the re-entry capsule HTV-R[13] for transportation from the international space station. For capsule-shaped vehicles, the effect of the high-temperature real-gas effect on aerodynamics is expected to be small compared to winged re-entry vehicles like the space shuttle. Nevertheless, precise aerodynamic characteristics of vehicles in a Hypersonic flow field are also necessary for vehicle stability, particularly for the pitching trim angle during lifting re-entry. To obtain the basic aerodynamic characteristics for the HTV-R option-2 configuration, a free-flight test in HIEST was performed to focus on trim-angle variation under high-temperature real-gas conditions.

The measurement systems for this test was the same as those of the blunted cone as described above and the schematics of an HTV-R option-2 6% scaled aerodynamic model used in this study were shown in Fig. 9. The diameter and the total mass of the model were 250mm and 20.1kg, respectively. When installing piezoelectric-type accelerometers, the model had a 50 × 50mm square open space vicinity of the model mass-centre. The magnetic model holder was redesigned for the HTV-R test model.

As shown in Fig. 10, the L/D and Pitching moment and angle of attack measured under HIEST low- and high-enthalpy conditions were compared to the results in HWT2. The trim angle of each test was 26 degrees (HWT2), 29 degrees (HIEST low-enthalpy) and 32 degrees (HIEST high-enthalpy), while the pitch-up trend at high enthalpy was consistent with real flight data[14]. However, through the uncertainty analysis, the PI-band for HIEST low and high-enthalpy condition were overlapped. It was therefore concluded that there was no significant difference on the trim angle between HIEST perfect gas and high-temperature real gas condition.

4.4. Lifting body

In 1996, the Hypersonic flight test for HYFLEX[15-16] lifting body was successfully conducted. It was intended to simulate the design, manufacturing, and flight of the Hypersonic lifting body vehicle and acquire Hypersonic flight data on aerodynamics, thermal protection system, and guidance and control. During the hypersonic flight, several data up to Mach 14 were obtained, including body flap (Elevon) efficiency, which was one of the crucial issues for vehicle stability during the Hypersonic gliding phase. To compare the aerodynamic characteristics between the flight and HIEST shock tunnel tests, the HYFLEX configuration was selected.

Fig. 11 (Top) shows the schematics of the HYFLEX 10% scaled aerodynamic model for the free-flight test. This model was made from stainless steel, 440mm long and weighing 18kg. Three onboard data recorders, capable of recording signals from 16CH accelerometers and 8CH pressure transducers (Fig. 11 Middle). Fig. 11(bottom) showed a picture taken in the first free-flight test with the HYFLEX model in HIEST.

Measured lift-drag ratio related to angle of attack (from 28 degrees to 52 degrees) were shown in Fig.12(left). In all the figures, square and triangle showed the results with elevon deflection angle 0 degrees and 20 degrees, respectively. Moreover, the open items and closed items were the results under perfect gas conditions and high-temperature real-gas conditions, respectively. The results measured in the conventional Hypersonic wind tunnel ONERA S4MA were also overlaid in all the figures as the solid (elevon 0 degrees) and dotted lines (elevon 20 degrees) to estimate the measurement accuracy of the present free-flight force measurements in HIEST. To estimate the measurement precision of the HIEST data, 95% (2-σ) PI (prediction interval) bands for the perfect gas condition and for the high-temperature real-gas condition were also plotted as the hatched area in the figures. As shown in these figures, S4MA measurements are inside the PI bands of HIEST measurements. It means that the measurements in HIEST agreed quite well with those of S4MA. These results revealed that drag force and lift force are insensitive to a stagnation enthalpy, namely flight speed in Hypersonic flow. These results also demonstrated the high-accuracy and precision of the present HIEST force measurement technique.

Fig. 12 (right) showed all the measured pitching moment coefficients in the present HIEST test results. Although the precision of the pitching moment was degraded than the drag or the lift force measurements, it was enough to determine the vehicle trim angle. For the discussion of the high-temperature real-gas effect on the longitudinal stability, HIEST measurements with an elevon deflection angle of 0 degrees are the focus. The regression analysis of the HIEST results indicated that the trim angle for HIEST perfect gas condition was estimated to 45 degrees. In contrast, it increased to about 55 degrees for the high-temperature real-gas condition. Forward movement of the pressure centre as

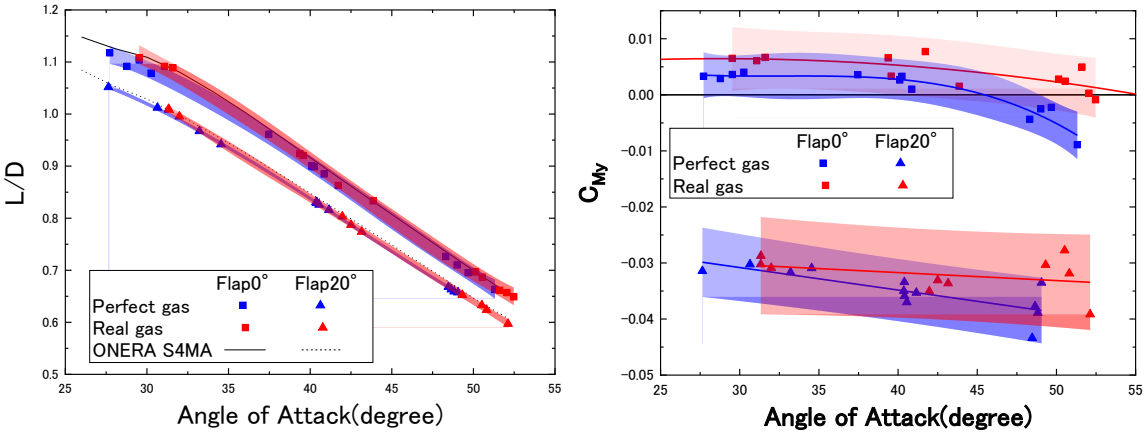

Fig 12. (Left) Lift-drag ratio of HYFLEX test model at angle of attack from 30 degrees to 50 degrees. Results measured in the conventional blow down wind tunnel ONERA-S4MAwere superimposed.

(Right) Pitching moment coefficient of HYFLEX test model at angle of attack from 30 degrees to 50 degrees. Results measured in the conventional blow down wind tunnel ONERA S4MA were overlapped.

a high-temperature real-gas effect was believed to be the cause of this significant difference of trim angle between the two free-stream test conditions in HIEST.

5. Conclusion

Aerodynamic characteristics for three generic reentry-vehicle configurations (blunted cone, capsule and lifting body) under high-temperature real-gas condition were reported. A free-flight force measurement technique developed for millisecond order short test duration was implemented to measure three-component aerodynamic characteristics in the free-piston high-enthalpy shock tunnel HIEST. Series of shock tunnel test campaigns revealed that the pitch trim angle increased rather than that of the perfect gas condition. The trend was remarkable with the lifting body model, which trend is suspected as an effect of the high-temperature real-gas.

Acknowledgement

The authors wish to thank Mr. Fujimura for cooperation on data reduction for the entire set of shots in this test campaign.

References

1. Young, J.C., Perez, L.F., Romere, P.O. and Kanipe, D.B.,: Space Shuttle Entry Aerodynamic Comparison of Flight 1 with Preflight Predictions, AIAA Paper No. 81-2476, (1981)
2. Maus, J.R., Griffith, B.J. Szema, K.Y. and Best, J.T.,: Hypersonic Mach Number and Real Gas Effects on Space Shuttle Orbiter Aerodynamics, J. Spacecraft & Rockets, Vol. 21, No. 2, 136-141, (1984)
3. Griffith, B.J., Maus, J.R., Majors, B.M. and Best, J.T.,: Addressing the Hypersonic Simulation Problem, J. Spacecraft & Rockets, Vol. 24, No. 4, 334-341, (1987)
4. Itoh, K., Ueda, S., Tanno, H., Komuro, T. and Sato, K.,: Hypersonic Aerothermodynamic and Scramjet Research Using High Enthalpy Shock Tunnel, Shock Waves, Vol. 12, 93-98, (2002)
5. Tanno, H., Komuro, T., Sato, K., Itoh, K. and Takahashi, M.,: Miniature data-logger for aerodynamic force measurement in impulsive facility, AIAA Paper No. 10-4204, (2010).
6. Bernstein, L.,: Force Measurement in Short-duration Hypersonic Facilities, AGARD-AG-214, edited by R.C. Pankhurst (Technical Editing and Reproduction, London), (1975).
7. Naumann,K.W., Ende,H., and Mathieu,G.: Millisecond aerodynamic force measurement with side-jet model in the ISL, Shock Waves 1:223-232, (1991)
8. Laurence, S.J. and Karl, S.: An improved visualization-based force-measurement technique for short duration hypersonic facilities, Experiments in Fluids, Vol.48, 6, (2010)
9. Laurence, S.J.: On tracking the motion of rigid bodies through edge detection and least-squares fitting, Experiments in Fluids, 52, No. 2 (2012)
10. Takahashi, M. et al.,: Influence of Thermal Non-Equilibrium on Nozzle Flow Condition of High Enthalpy Shock Tunnel HIEST, AIAA Pap. 09, 7267 (2009)
11. Watari, M. et al.,: Flow Qualities of JAXA Hypersonic Wind Tunnel Facilities, AIAA Pap. 06, 8047 (2006)
12. https://www.onera.fr/windtunnel/s4ma

13. Imada,T.,: Concept and Technology of HTV-R: An Advanced Type of H-II Transfer Vehicle, to be published in the Proceedings of ISTS-2011(2011)
14. Tran, Ph., Paulat, J.C. and Boukhobza, P.: Re-entry flight experiments lessons learned – The atmospheric reentry demonstrator ARD, NATO-RTO-EN-AVT-130, (2005)
15. Shirouzu,M. and Yamamoto,M.,: Overview of the HYFLEX project, AIAA Pap. 96, 4524(1996)
16. Watanabe, S. et al.,: Aerodynamic characteristics evaluation of hypersonic flight experiment (HYFLEX) vehicle based on flight data, AIAA Pap. 96, 4527(1996)